NACA

RESEARCH MEMORANDUM

FLUTTER EXPERIENCES WITH THIN POINTED-TIP WINGS DURING FLIGHT TESTS OF ROCKET-PROPELLED MODELS AT MACH NUMBERS FROM 0.8 TO 1.95

By Harvey A. Wallskog

Langley Aeronautical Laboratory
Langley Field, Va.

NATIONAL ADVISORY COMMITTEE
FOR AERONAUTICS

WASHINGTON
April 4, 1955

NATIONAL ADVISORY COMMITTEE FOR AERONAUTICS

RESEARCH MEMORANDUM

FLUTTER EXPERIENCES WITH THIN POINTED-TIP WINGS DURING FLIGHT TESTS OF ROCKET-PROPELLED MODELS AT MACH NUMBERS FROM 0.8 TO 1.95

By Harvey A. Wallskog

SUMMARY

Flutter data were obtained over the Mach number range from 0.8 to 1.95 from free-flight tests of several wing-body combinations which were part of a general zero-lift drag investigation. All of the wings tested had NACA $65_{(06)}$A003 streamwise airfoil sections and the plan-form variations consisted of delta wings with aspect ratios of 3 and 4, diamond wings with aspect ratios of 2.3 and 3, and an arrow wing with aspect ratio of 3.2. Time histories of model speed, Mach number, and air density are presented for each model along with flutter frequency, amplitude, and reduced-frequency parameter plotted as functions of model speed.

The results show that pointed-tip wings of high overall static strength may possess poor flutter characteristics. It is believed that the present results were significantly affected by the method of construction used (that is, the effects of distribution of material in laminated wood-metal construction). A correlation of the present results and other available triangular-wing flutter data was made and compared with the flutter boundary developed by Martin in NACA RM L51J30. Although insufficient data were available to establish a boundary for all pointed-tip wings, it is believed that these data may be useful to a designer in comparing his design to others which did or did not experience flutter.

INTRODUCTION

Tests of thin delta-, diamond-, and arrow-plan-form wings have illustrated the low zero-lift drag characteristics desirable for transonic and supersonic flight. Current developments in delta-wing-airplane and missile configurations have stimulated interest in flutter information for such plan-form wings. The flutter data contained herein were obtained

from models which were part of a general zero-lift drag investigation (ref. 1) and were intended to provide high Reynolds number zero-lift drag coefficients of thin wings (NACA $65_{(06)}$A003 airfoil section) of various plan forms. Since flutter was not anticipated in this program, the instrumentation used to determine the frequency and approximate amplitude of the vibration was limited to a normal accelerometer located within the fuselage of each model. These rocket-propelled models were designed and fabricated by methods proved previously to give high overall static strength.

It is believed that, on the basis of the comparison made using the criterion developed by Martin in reference 2, the data presented herein will be of interest and may serve in some capacity as a guide in future design work. These data also supplement existing experimental information and may prove useful when theoretical techniques are perfected.

SYMBOLS

S	total wing area obtained by extending the leading and trailing edges to the body center line, sq ft
S_b	body frontal area, sq ft
A	aspect ratio of total wing
$\bar{c}$	mean aerodynamic chord, ft
V	model airspeed, ft/sec
M	Mach number
ρ	free-stream air density, slugs/cu ft
$\bar{X}$	empirical flutter criterion, $\frac{p}{p_o}\left(\frac{\lambda + 1}{2}\right)\left(\frac{A_p^3}{A_p + 2}\right)\frac{39.3}{(t/c)^3}$, lb/sq in.
p/p_o	ratio of local atmospheric pressure to sea-level standard pressure
λ	wing taper ratio
A_p	aspect ratio of one exposed wing panel

c	streamwise wing chord at 50 percent of exposed span outboard on the exposed wing panel, in.
t	maximum airfoil thickness at c, in.
G_E	effective shear modulus of wing structure calculated from $\frac{(JG)_{wood} + (JG)_{metal}}{J_S}$, lb/sq in.
J_S	section torsional constant, approximately $4I_{airfoil}$, $in.^4$
$I_{airfoil}$	section moment of inertia, approximately $0.0377ct^3$, $in.^4$
f	measured flutter frequency, cycles/sec
ω	measured flutter frequency, radians/sec
a	estimated amplitude of model vibration in normal acceleration, g units ± from trim
k	reduced-frequency parameter, $\omega\bar{c}/2V$

MODELS AND TESTS

Drawings of the five rocket-propelled models are presented in figure 1 which illustrates their general arrangement and dimensional details. Photographs of the models appear in figure 2. The fuselage shape (common to all models) was generated by parabolic segments having their vertices at 40 percent of the fuselage length. The fuselage ordinates for models 1 to 4 are presented in table I. The fuselage of model 5 was one-half scale of those used for models 1 to 4. The five wing plan forms tested are as follows:

Model	Plan form	Aspect ratio, A
1	52.5° delta	3.07
2	45° delta	4.0
3	Diamond	2.31
4	Diamond	3.07
5	Arrow	3.2

The 50-percent-chord line of each diamond wing had 0° sweepback and the leading edge of the arrow wing was swept 55°. For each wing the airfoil

section in the streamwise direction was an NACA $65_{(06)}$ A003 airfoil section. Airfoil ordinates are presented in table II. Weight, balance, and other pertinent data are listed in table III for each model.

Presented in figure 3 are drawings which show details of wing material and construction. In the fabrication of the wings, urea-formaldehyde glue was used for all wood joints and 1/32-inch-thick birch veneer was cyclewelded to both sides of each metal insert prior to assembly. Material used in the wing construction consisted of laminated mahogany with inserts and inlays of 2024-T3 aluminum alloy (formerly designated 24S-T3). As illustrated by the magnitudes of the design ultimate loads presented in table III, this method of construction provided wings of high overall static strength.

Two-stage propulsion systems consisting of solid-fuel rocket motors were used to propel models 1, 2, 4, and 5 to supersonic speeds and altitudes up to 20,000 feet. The propulsion system of model 3 consisted of an internal rocket motor only. With the exception of model 1, all models were launched and flew initially at elevation angles of 60°. Model 1 was launched at 60°, but the flight-path angle decreased rapidly producing a rather shallow flight path. (Maximum altitude was about 1,500 feet.)

Time histories of model velocity and altitude were obtained from a CW Doppler radar unit and an NACA modified SCR 584 tracking radar unit. Radiosonde units provided additional information necessary to determine Mach numbers and air density. In addition, each model was equipped with a telemeter which transmitted continuous measurements from instruments located within the fuselage. The only telemeter data utilized in the present paper were that from the normal accelerometer which was located in the fuselage of each model near the center of gravity.

The telemeter record obtained during the flight test of each model showed a high-frequency oscillation present on the trace of normal acceleration from the accelerometer in the fuselage over a considerable portion of the record. Previous tests with models which were instrumented for wing flutter and which contained a normal accelerometer within the fuselage have indicated that in almost all cases the accelerometer (and recorder galvanometer) was capable of recording the flutter oscillation. For this reason, and because the instrumented bodies of the present type have been flown with various wings which did not encounter this type of vibration (ref. 1), the oscillations recorded during the present tests are attributed to wing flutter. The flutter oscillation appears on the record at the correct frequency but generally at reduced amplitudes. The actual amplitudes were calculated from recorded amplitudes for each model using the natural frequency and damping ratio of the individual instruments and galvanometers and standard response curves for linearly damped systems. The resulting calculated amplitudes are not particularly accurate because of the uncertainty in the damping ratios of the accelerometers

and galvanometers and because the flutter oscillation is not always sinusoidal but sometimes contains harmonics. The presence of harmonics in the flutter oscillation would cause the calculated amplitudes to be low.

Presented in figure 4 and table IV are the results of tests conducted to determine the natural frequencies of vibration of the wings. The frequency and approximate node pattern for several natural modes are presented for models 2, 4, and 5. These data were obtained with each complete model suspended in loops of elastic cord and an electromagnetic shaker attached to the fuselage near the model center of gravity. Only the frequency of the first natural mode was obtained for models 1 and 3.

RESULTS AND DISCUSSION

As illustrated in figure 5 flutter began at maximum speed for models 1 and 3 and continued until the models decelerated to transonic speeds. Thus, for models 1 and 3 it appears that the relatively high longitudinal acceleration delayed the onset of flutter. Data from models 2, 4, and 5, however, showed that flutter began during the accelerating portion of the flight tests at transonic speeds and continued through maximum speed and until the models decelerated to high subsonic speeds. Wing failure did not occur during any of the present tests, and the models flew without incident at subsonic speeds after the flutter stopped.

Presented in figure 6 are values of flutter frequency f, amplitude a, and reduced-frequency parameter $k = \frac{\omega \bar{c}}{2V}$ for each model plotted as functions of model speed. For the 52.5° delta wing of model 1, there were no abrupt changes in f, a, or k throughout the speed range. The data from model 2, the 45° delta wing, showed that f and k varied smoothly through the speed range, whereas abrupt changes occurred in amplitude. For model 3, the lower aspect-ratio diamond wing, there were small irregularities in frequency, but both k and a were relatively smooth during the decelerating portion of the flight. The flutter data from model 4 were more irregular throughout the speed range. A rather abrupt change in frequency shortly after maximum speed indicated a change in flutter mode. Another change in f, smaller but more abrupt, occurred at $V \approx 1{,}400$. These two changes in f occurred near the third and second natural modes, respectively. There were marked changes in the amplitude of the model oscillation throughout the speed range. The values of f and k from model 5 varied smoothly over the speed range. The amplitude of the model oscillation is shown for decelerating flight only because of the large irregularities which occurred during the

accelerating portion. The amplitudes of the model oscillations presented for models 1, 3, and the low-speed part of model 4 are probably low because of the presence of harmonics.

In 1951, Martin (ref. 2) developed a criterion in which significant parameters were grouped in an attempt to establish limits of the critical values of the structural and aerodynamic requirements for a wing to be flutter-free. This criterion was based on modifications to an approximate flutter formula which was intended for heavy high-aspect-ratio wings having a low ratio of bending to torsional frequency. The large quantity of data correlated in reference 2 showed that two regions can be defined in which the flutter and no-flutter test points are reasonably well separated. By using these data, Martin was able to establish a flutter boundary for unswept and swept wings with finite tip chords and bending-torsion-type flutter. The application of modifications to this formula to include low-aspect-ratio wings including swept and highly tapered wings was, admittedly, stretching the basic formula; however, the parameters were adjusted until there seemed to be a reasonable coherence in the results.

The test points contained in figure 7 represent delta-, diamond-, and arrow-plan-form wings correlated by using the same criterion developed by Martin. In figure 7 the ordinate $\bar{X}$ represents a plan-form thickness and altitude parameter and the abscissa G_E is the effective torsional shear modulus of the wing structure. The value of $\bar{X}$ in the present paper is equivalent to $\frac{p}{p_o}\left(\frac{\lambda + 1}{2}\right)X$ in reference 2. The experimental data of figure 7 were obtained from tests conducted in wind tunnels (refs. 3 and 4) and free-flight rocket-propelled model tests (refs. 5 and 6). Models 1 to 5 of the present paper correspond to test points 1 to 5, respectively, in figure 7. For each wing the value of G_E was calculated at a streamwise section 50 percent outboard on the exposed wing panel. For the wings which were laminated of wood and metal, the calculated value of G_E is by necessity an overall, average value. An additional factor which injects a degree of uncertainty in the results is the value of thickness ratio to use for the wings of reference 3. These tests utilized solid metal wings which were flat plates with beveled leading and trailing edges. For these test points, the values of G_E were known and the value of $\bar{X}$ was determined by using the thickness ratio at the 50-percent outboard station on the exposed wing panel.

In figure 7 the points labeled 1 to 7 represent wings which were built-up structures of wood and metal, with considerable variation in the size and shape of the metal portions. Because of this, the stiffness of

the wings varied widely both chordwise and spanwise, and resulted generally in wings with relatively weak flexible-tip and trailing-edge portions.

The solid points labeled 6 in figure 7 illustrate the effect that weak, flexible portions of the wing have on the flutter characteristics of a particular plan form. The two wings corresponding to the two points were identical in size and shape. The difference in the wings of the two tests was that the inboard, forward portion of one wing (the point on the right) was made substantially stiffer by the use of steel upper and lower surface inlays. A considerable portion of the tip and trailing edge, however, was left very flexible. The results of these tests showed that, despite the increase in the overall stiffness of the second wing, the two wings fluttered over approximately the same speed range.

Another illustration in figure 7 of the effect of discontinuities in stiffness over the wing is the comparison of the solid test point labeled 7 and the open point adjacent to it. The delta wing which experienced flutter was constructed of laminated wood with a single, thin, metal insert which was approximately the size and shape of the control surface. Because the control surface was deflected a small amount, the inboard end was not secured to the fuselage, thus leaving the entire trailing edge extremely flexible. The wing that did not flutter had a larger value of t/c, a comparatively thick trailing-edge metal insert, and, in addition, metal upper and lower surface inlays. Thus, it appears that the marked difference in trailing-edge flexibility may have been the reason for the different test results.

From the previously mentioned considerations, it is believed that, although the weak, flexible wing tip and trailing-edge portions had very little influence in the calculation of G_E, they had a pronounced effect on flutter characteristics. It appears from the results of the two models labeled 6 and the one labeled 7 that all the points representing models 1 to 7 should appear in figure 7 at somewhat lower values of G_E depending on the degree and extent of the weak, flexible portions. Therefore, the boundary of reference 2 appears to be conservative for pointed-tip wings of fairly uniform structural characteristics. The open points which lie above the boundary represent wings of more uniform construction and provide additional evidence that the boundary is conservative. Unfortunately, as a result of insufficient data it was impossible to establish a boundary as unique as in reference 2; however, the fact that the boundary of reference 2 appears conservative would make it useful for most engineering purposes. In general, the results show that pointed-tip wings of high overall static strength may possess poor flutter characteristics.

CONCLUDING REMARKS

Flutter was experienced by several wing-body combinations which were tested in free flight over the Mach number range from 0.8 to 1.95 as part of a general zero-lift drag investigation. The five wings tested were delta wings with aspect ratios of 3 and 4, diamond wings with aspect ratios of 2.3 and 3, and an arrow wing with an aspect ratio of 3.2, all with NACA $65_{(06)}$A003 streamwise airfoil sections.

The results show that pointed-tip wings of high overall static strength may possess poor flutter characteristics. It appears that the results from the present test configurations may have been caused by or at least influenced by the presence of relatively weak wing-tip and trailing-edge portions.

Langley Aeronautical Laboratory,
National Advisory Committee for Aeronautics,
Langley Field, Va., January 11, 1955.

REFERENCES

1. Morrow, John D., and Nelson, Robert L.: Large-Scale Flight Measurements of Zero-Lift Drag of 10 Wing-Body Configurations at Mach Numbers From 0.8 to 1.6. NACA RM L52D18a, 1953.

2. Martin, Dennis J.: Summary of Flutter Experiences As a Guide to the Preliminary Design of Lifting Surfaces on Missiles. NACA RM L51J30, 1951.

3. Tuovila, W. J.: Some Wind-Tunnel Results of an Investigation of the Flutter of Sweptback- and Triangular-Wing Models at Mach Number 1.3. NACA RM L52C13, 1952.

4. Herr, Robert W.: A Preliminary Wind-Tunnel Investigation of Flutter Characteristics of Delta Wings. NACA RM L52B14a, 1952.

5. Lauten, William T., Jr., and Judd, Joseph H.: Supersonic Flutter of a 60° Delta Wing Encountered During the Flight Test of a Rocket-Propelled Model. NACA RM L54D12a, 1954.

6. Lauten, William T., Jr., and Mitcham, Grady L.: Note on Flutter of a 60° Delta Wing Encountered at Low-Supersonic Speeds During the Flight of a Rocket-Propelled Model. NACA RM L51B28, 1951.

TABLE I

FUSELAGE ORDINATES FOR MODELS 1 TO 4

Axial distance measured from nose point, in.	Radius, in.
0	0
1.0	.247
2.0	.490
3.0	.728
5.0	1.190
7.0	1.632
10.0	2.259
16.0	3.385
22.0	4.336
28.0	5.115
34.0	5.721
40.0	6.154
46.0	6.414
52.0	6.500
58.0	6.481
64.0	6.423
70.0	6.325
76.0	6.190
82.0	6.016
88.0	5.803
94.0	5.552
100.0	5.262
106.0	4.933
112.0	4.565
118.0	4.159
124.0	3.714
130.0	3.230

TABLE II

NACA $65_{(06)}$A003 AIRFOIL ORDINATES

Station, percent chord	Ordinate, percent chord
0	0
.5	.2320
.75	.2815
1.25	.3590
2.5	.4905
5.0	.6565
7.5	.7955
10	.9120
15	1.0970
20	1.2370
25	1.3435
30	1.4210
35	1.4725
40	1.4980
45	1.4960
50	1.4625
55	1.3965
60	1.3010
65	1.1820
70	1.0435
75	.8875
80	.7185
85	.5415
90	.3635
95	.1850
100	.0065
L.E. radius: 0.0573 T.E. radius: 0.0035	

TABLE III

WEIGHT, BALANCE, INERTIA, AND STRUCTURAL

DATA FOR THE ROCKET-PROPELLED FREE-FLIGHT MODELS

	Model				
	1, 52.5° delta	2, 45° delta	3, diamond (A = 2.31)	4, diamond (A = 3)	5, arrow (A = 3.2)
Total weight, lb					
With fuel	427.5	422.2	348.2	344.6	64.0
Empty	330.3	325.0	250.5	248.4	54.75
Wing loading, lb/ft^2					
With fuel	14.2	14.0	22.9	22.8	21.3
Empty	10.9	10.8	16.5	16.3	18.2
Center of gravity from nose, in.					
With fuel	72.3	71.8	66.7	72.8	38.3
Empty	71.2	70.6	65.1	71.5	38.0
Moment of inertia, I_Y, slug-ft^2					
With fuel	-----	93.4	------	70.8	-----
Empty	86	82.1	65.3	59.5	3.2
Calculated weight of one exposed wing panel, lb	55.6	52.3	12.2	18.6	2.38
Design ultimate load of wing in bending, lb/ft^2	810	610	900	1760	530
Section effective stiffness parameter, EI/c^4, lb/in.^{2}	3.5	3.5	2.1	3.7	1.1

TABLE IV

FREQUENCIES OF VIBRATION OBTAINED FROM PREFLIGHT SHAKE TESTS FOR MODELS 1 TO 5

Mode	Frequency, cps				
	Model 1	Model 2	Model 3	Model 4	Model 5
First	29	22	70	52	51
Second	--	48	--	87	142
Third	--	80	--	134	218
Fourth	--	123	--	152	---
Fifth	--	144	--	172	---
Sixth	--	---	--	186	---

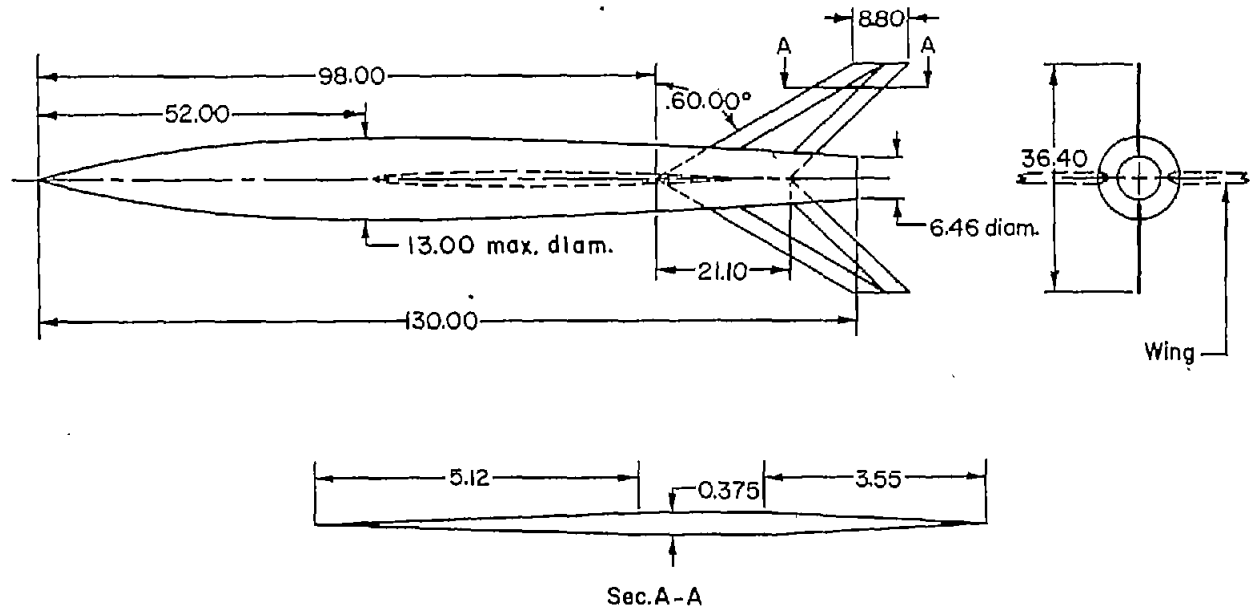

(a) Dimensional details of fuselage and stabilizing fins. Same for models 1 to 4. Dimensions of model 5 are one-half scale of those shown.

Figure 1.- General arrangement of rocket-propelled models. All dimensions are in inches.

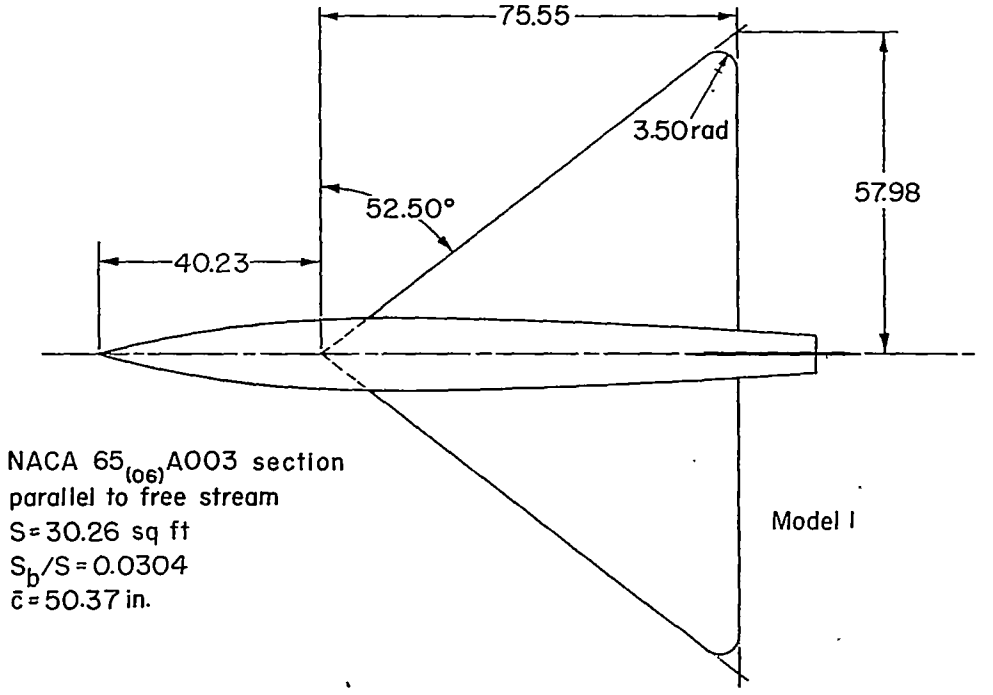

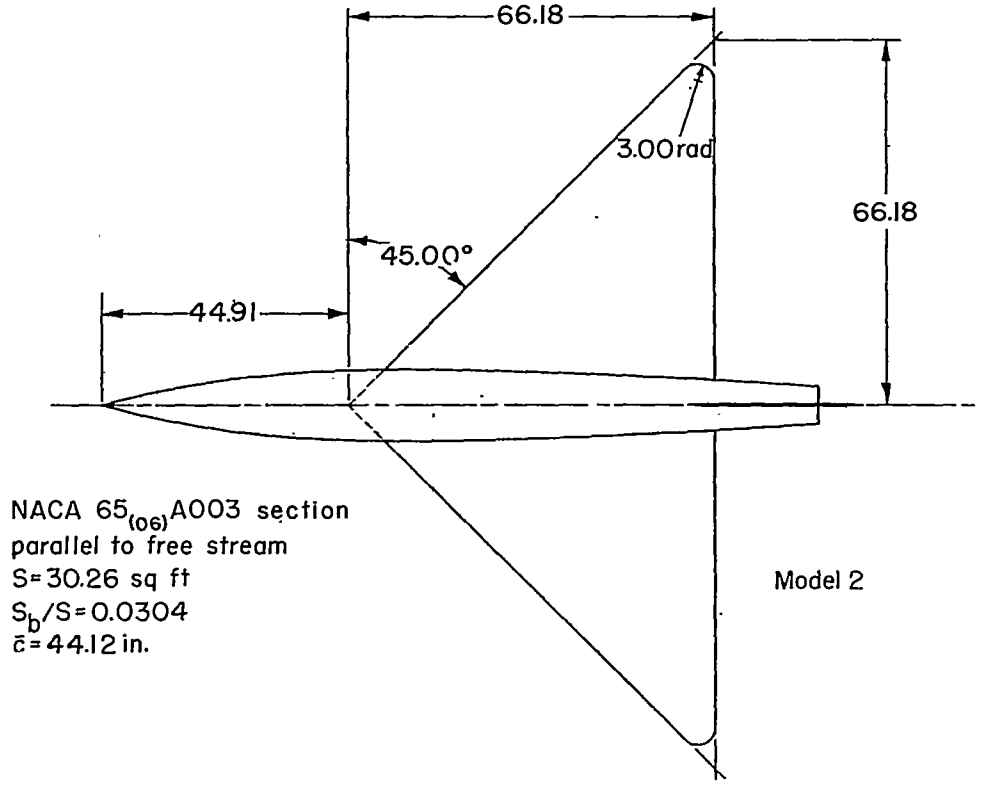

(b) Dimensional details of the delta-wing configurations, models 1 and 2.

Figure 1.- Continued.

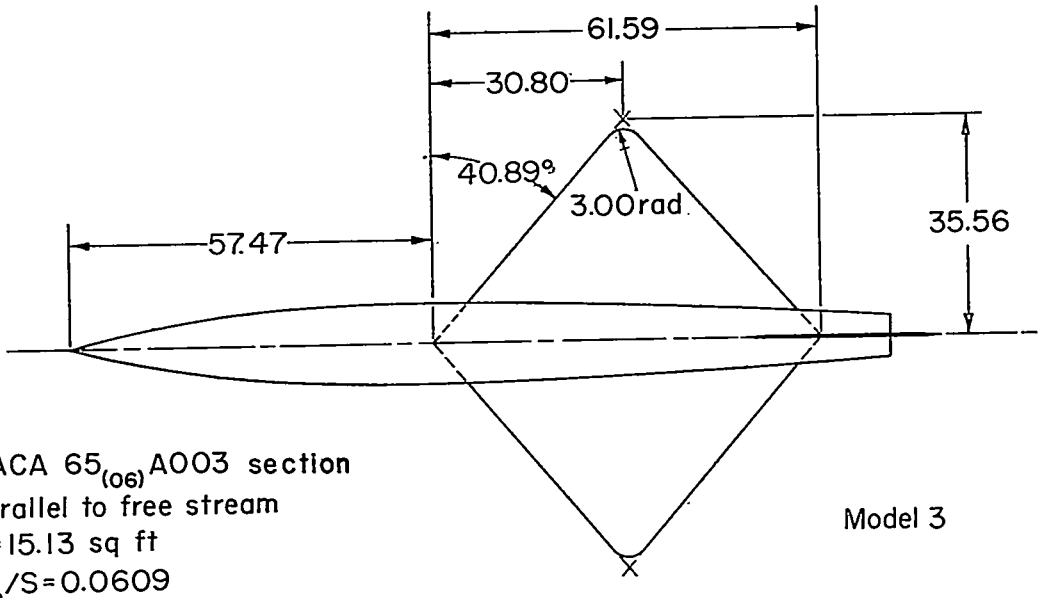

NACA $65_{(06)}$A003 section
parallel to free stream
S = 15.13 sq ft
$S_b/S = 0.0609$
$\bar{c}$ = 41.06 in.

Model 3

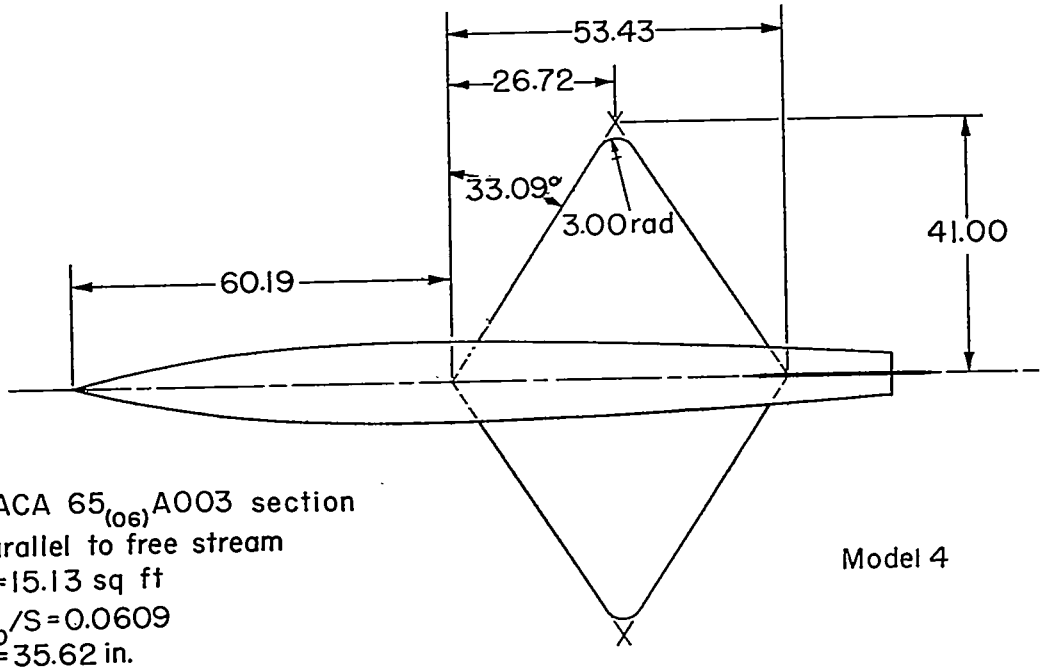

NACA $65_{(06)}$A003 section
parallel to free stream
S = 15.13 sq ft
$S_b/S = 0.0609$
$\bar{c}$ = 35.62 in.

Model 4

(c) Dimensional details of the diamond-wing configurations, models 3 and 4.

Figure 1.- Continued.

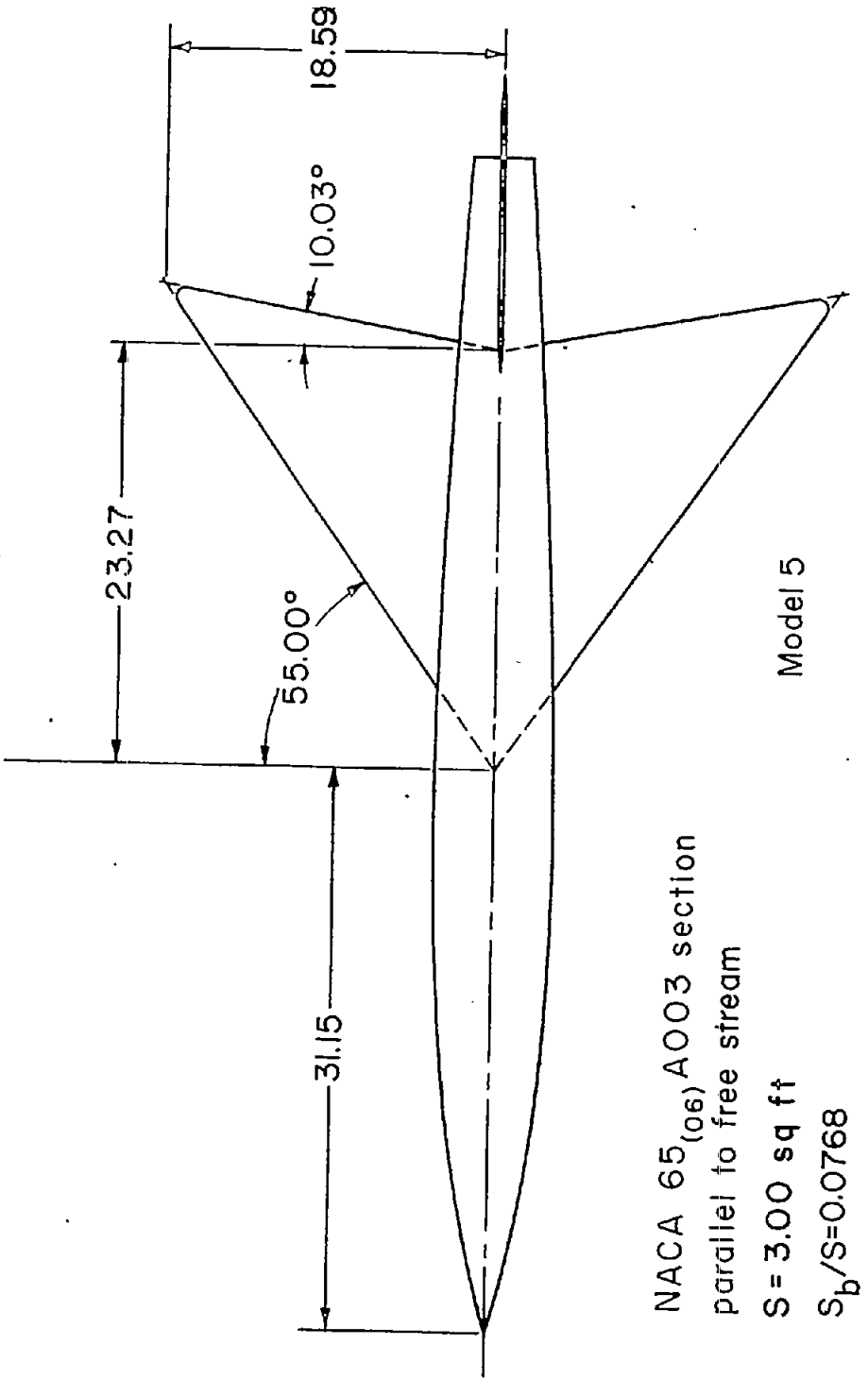

(d) Dimensional details of the arrow-wing configuration, model 5.

Figure 1.- Concluded.

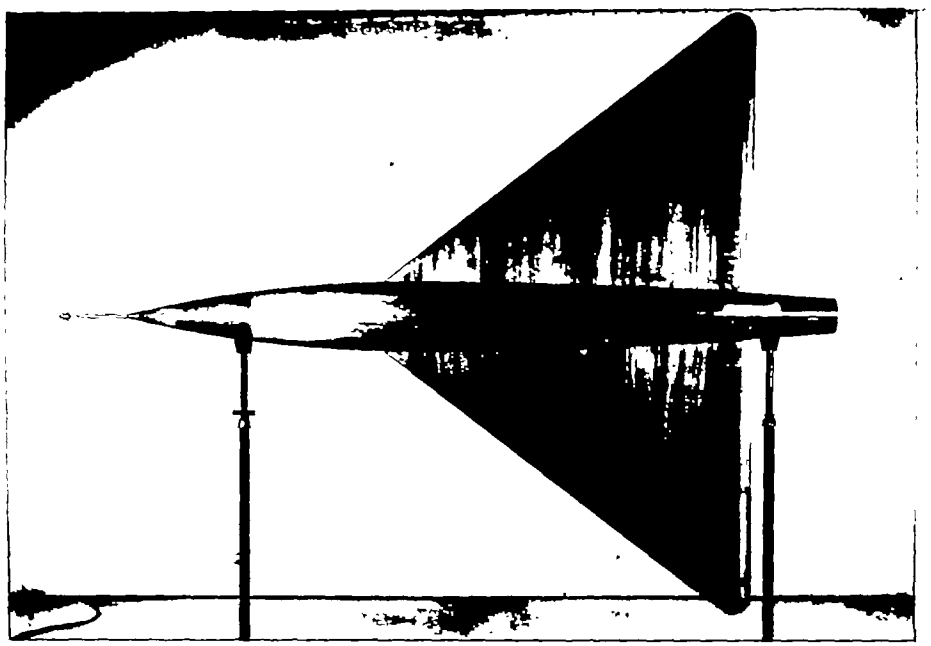

Model 1. L-75320.1

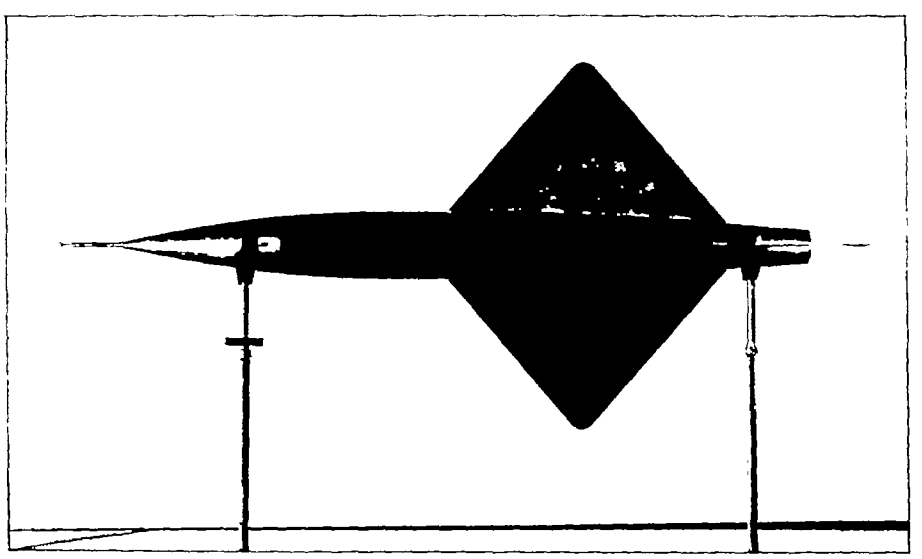

Model 3. L-72145.1

(a) Models 1 and 3.

Figure 2.- Photographs of the rocket-propelled models.

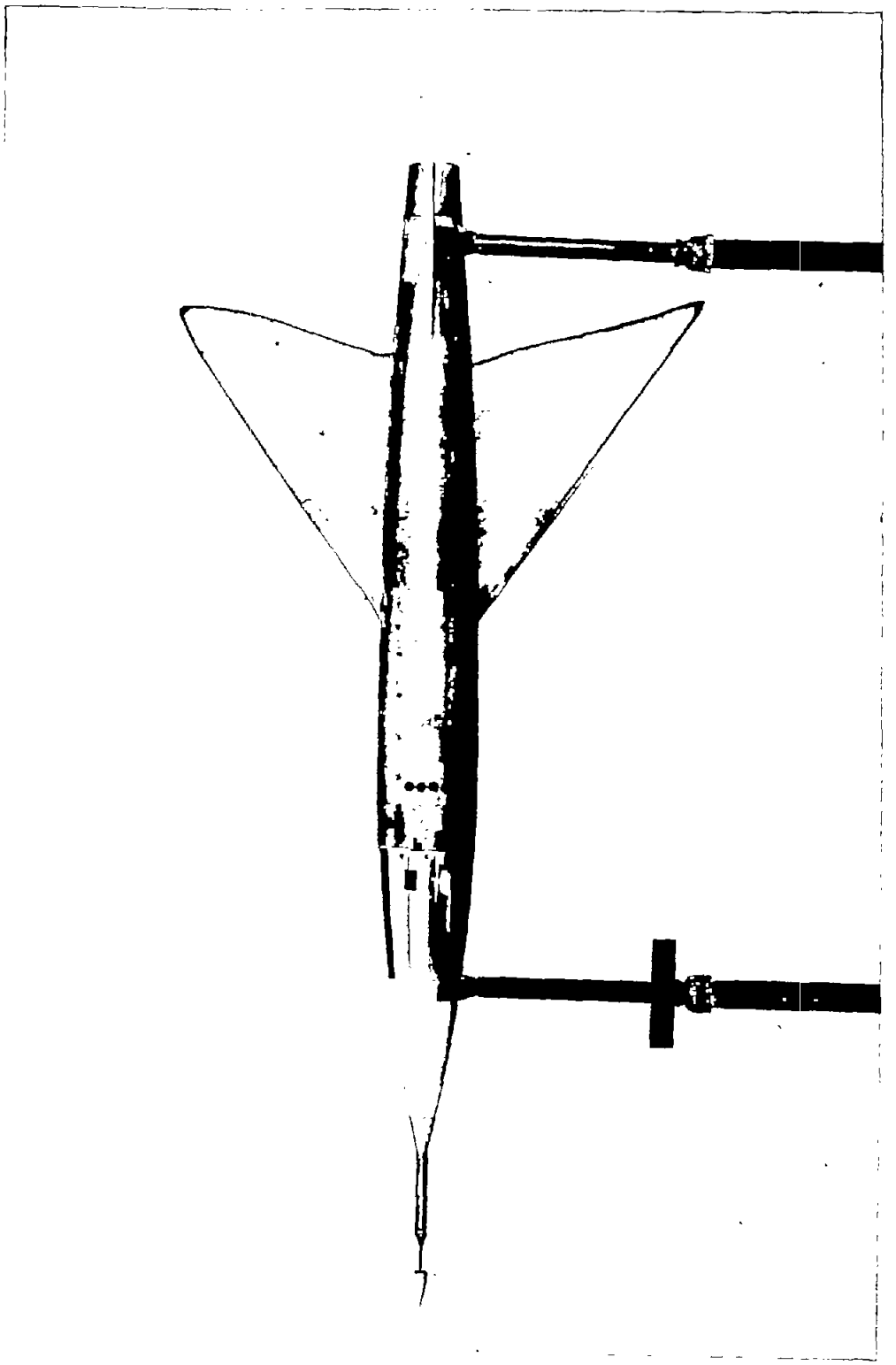

L-81617.1

(b) Model 5.

Figure 2.- Concluded.

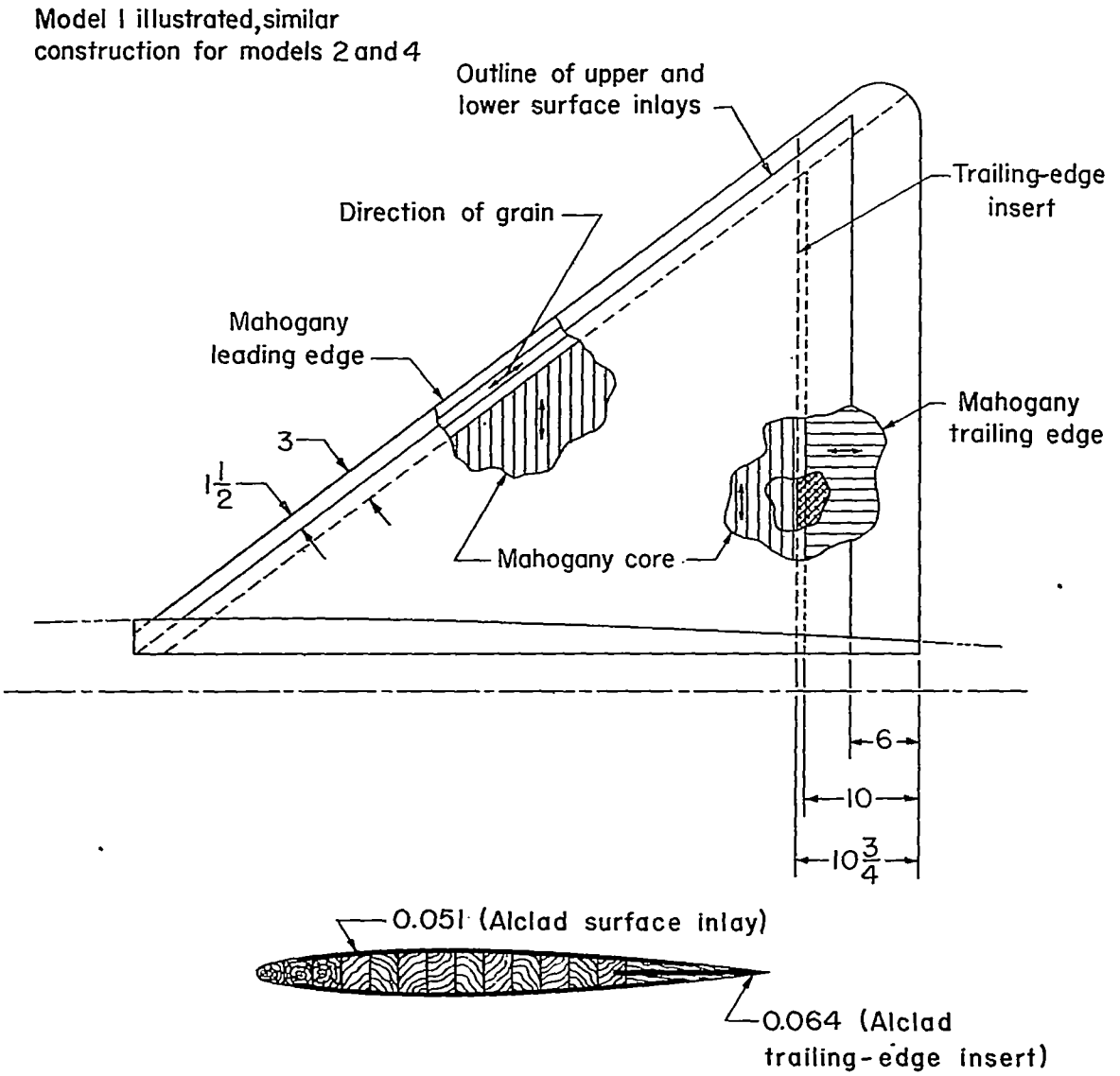

(a) Models 1, 2, and 4.

Figure 3.- Details of wing construction and materials. All dimensions are in inches.

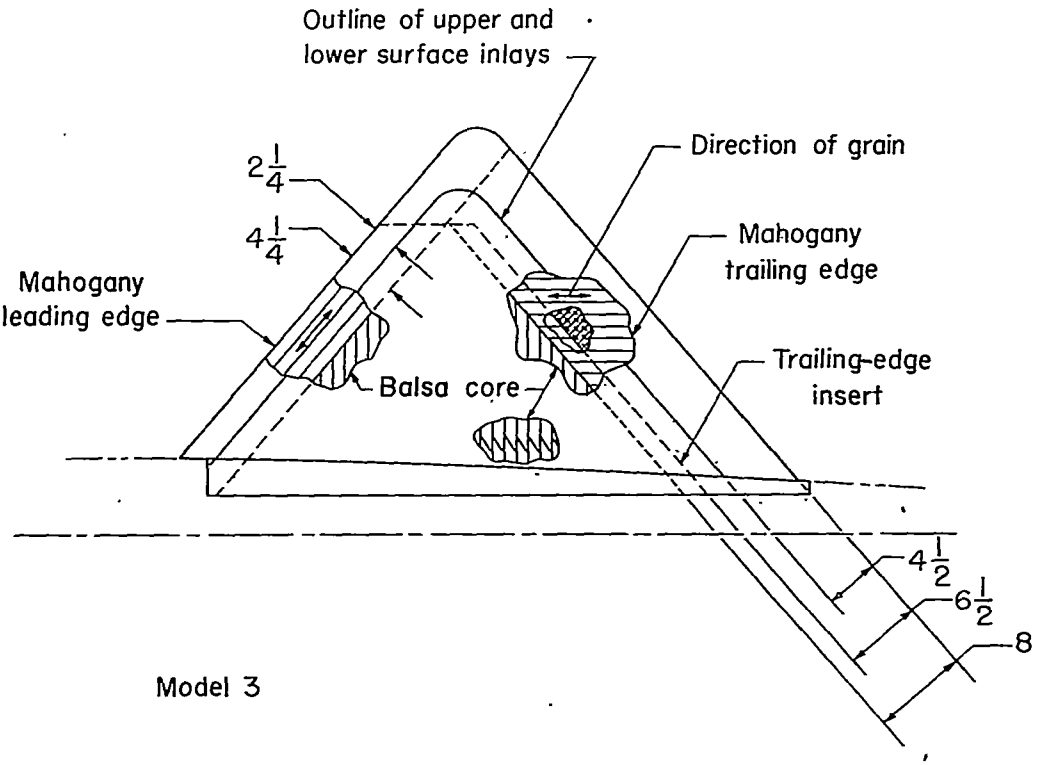

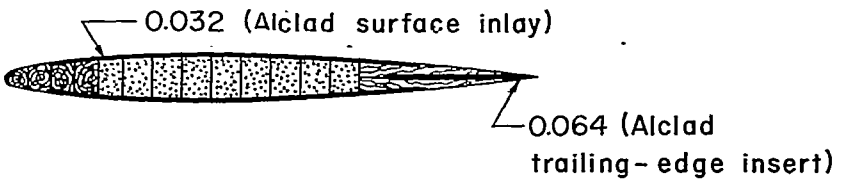

Typical streamwise section, not to scale

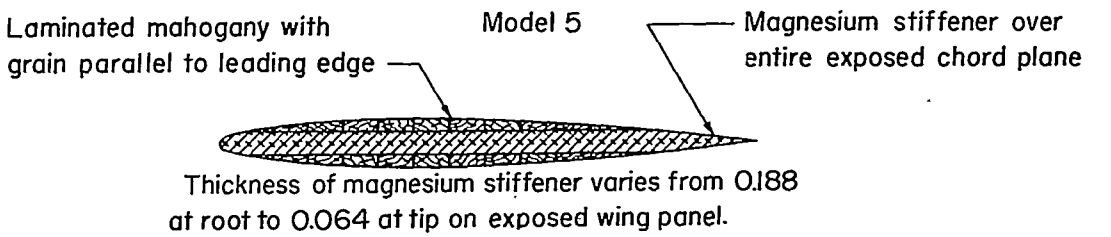

Typical streamwise section, not to scale.

(b) Models 3 and 5.

Figure 3.- Concluded.

[redacted]

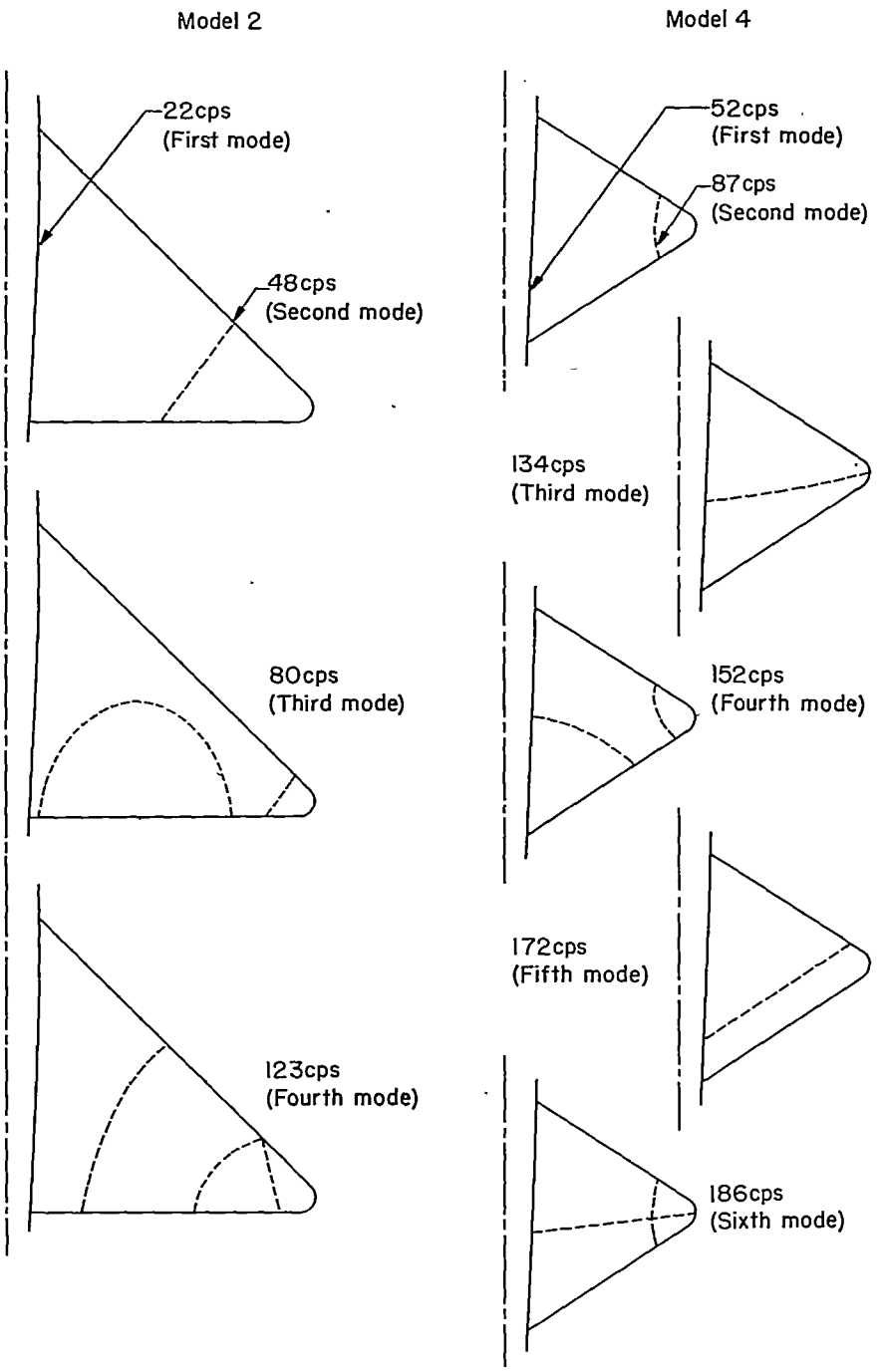

(a) Models 2 and 4.

Figure 4.- Frequencies of vibration and approximate node patterns obtained from preflight shake test.

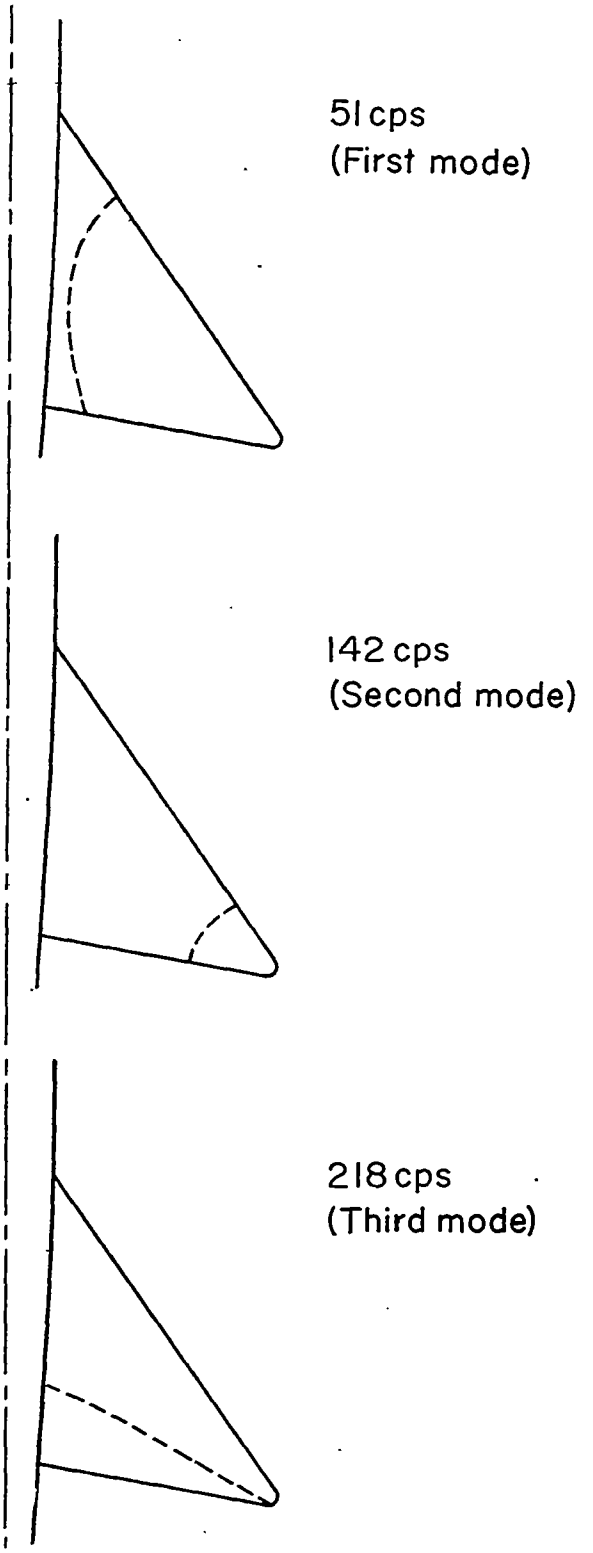

(b) Model 5.

Figure 4.- Concluded.

[redacted]

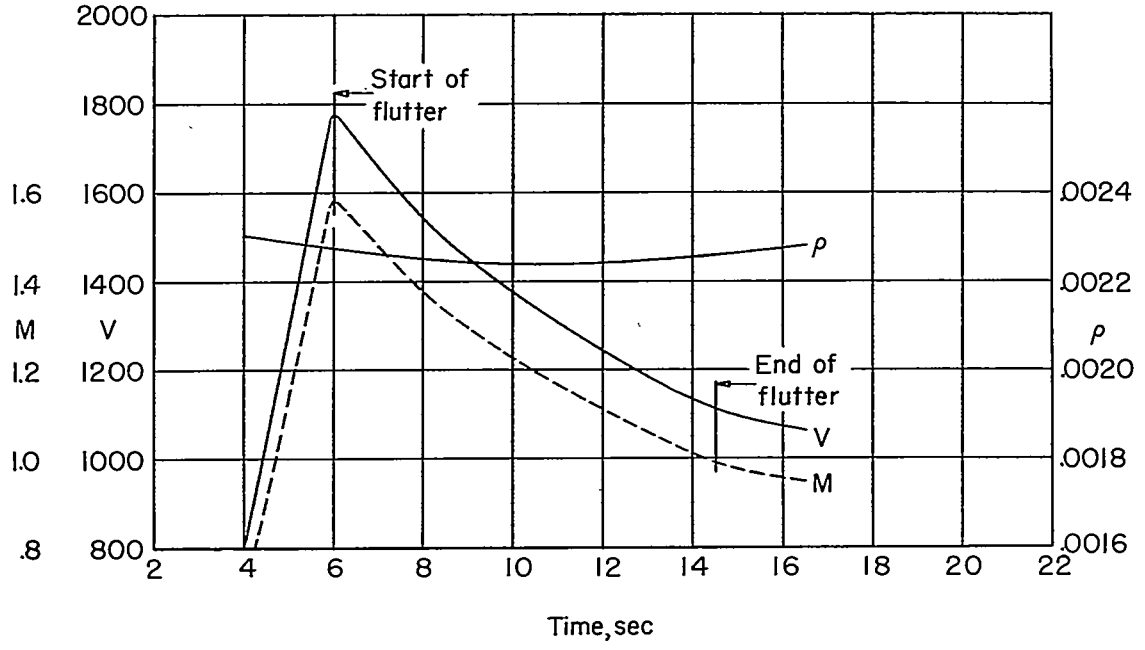

(a) Model 1 - delta wing (A = 3.07).

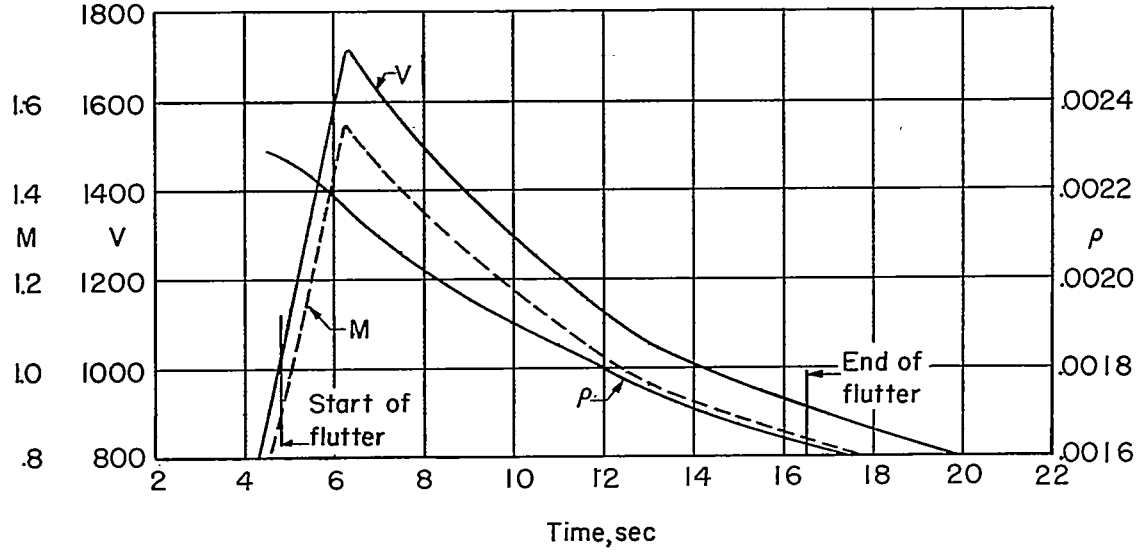

(b) Model 2 - delta wing (A = 4.0).

Figure 5.- Variation of model speed, Mach number, and air density with time showing the range during which flutter occurred.

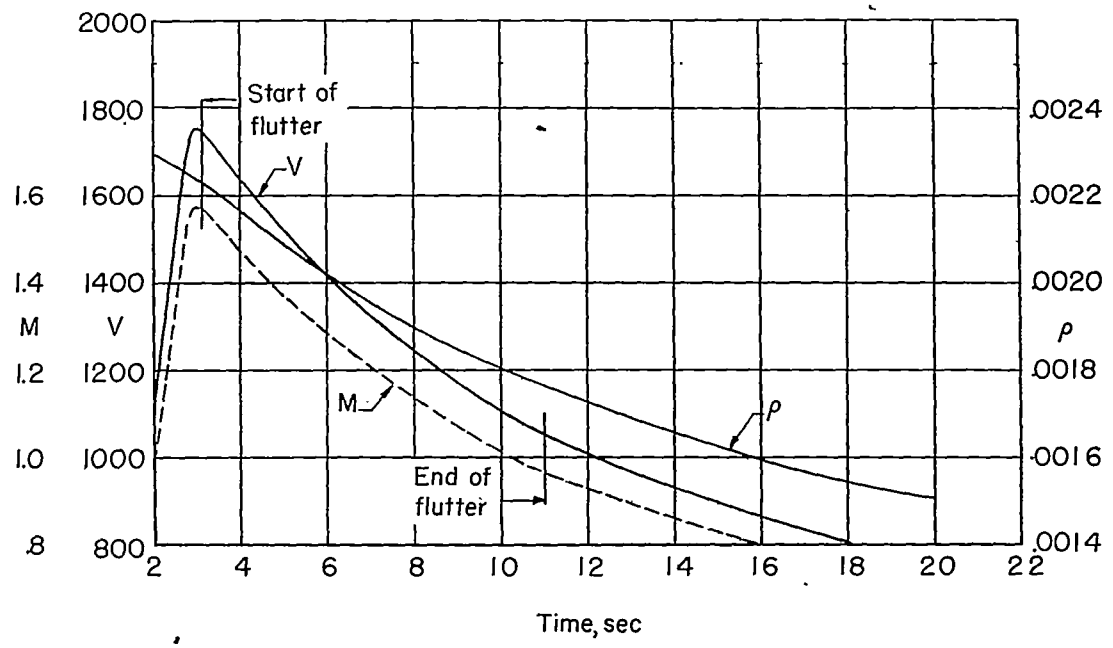

(c) Model 3 - diamond wing (A = 2.31).

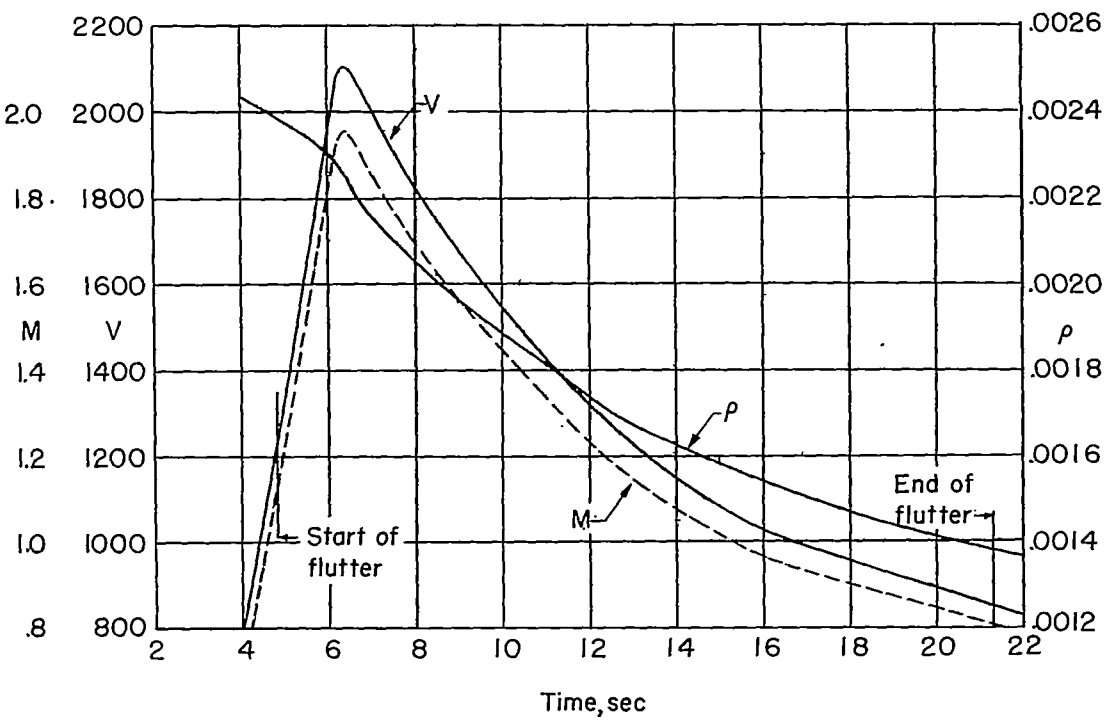

(d) Model 4 - diamond wing (A = 3.07).

Figure 5.- Continued.

[redacted]

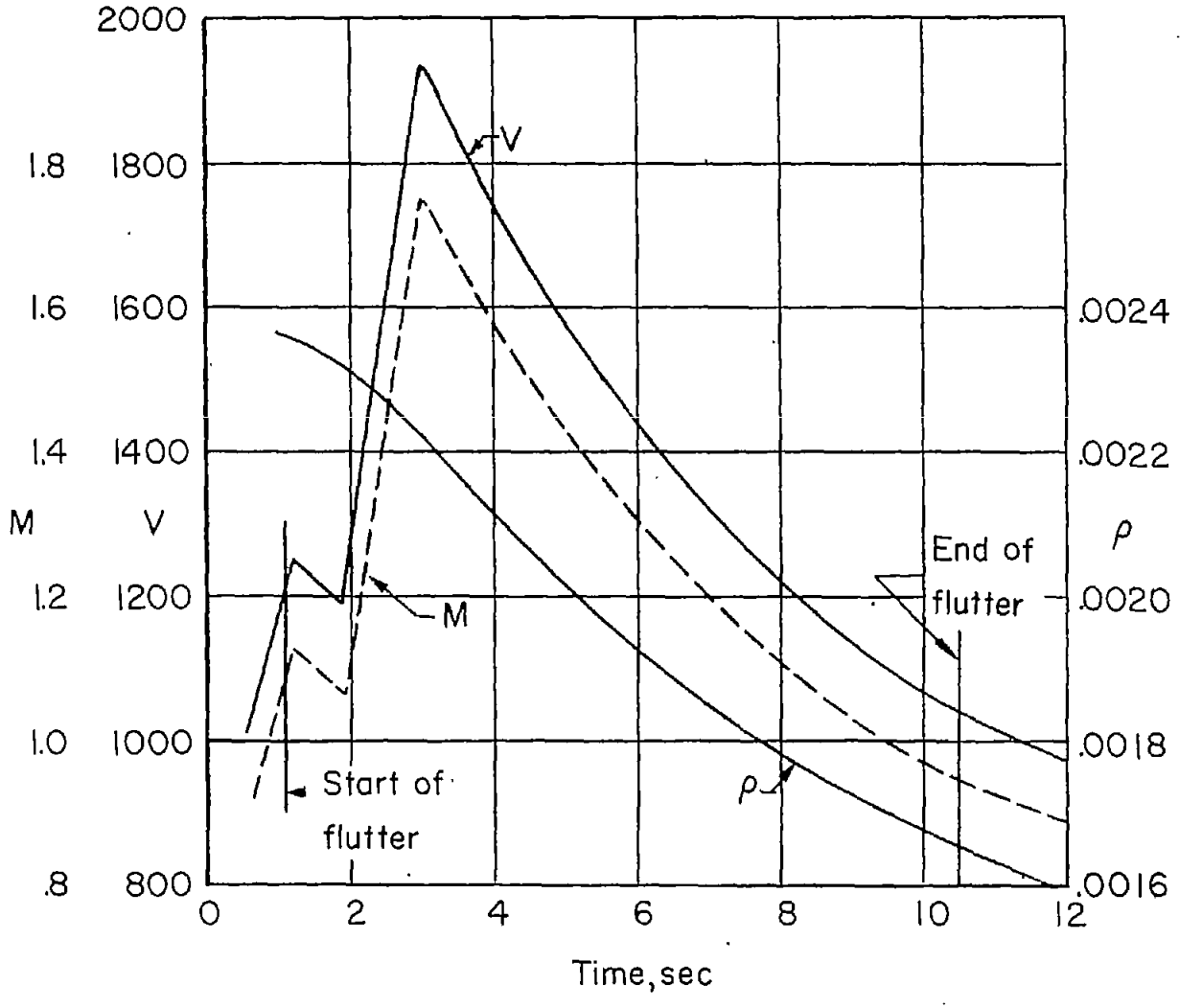

(e) Model 5 - arrow wing (A = 3.2).

Figure 5.- Concluded.

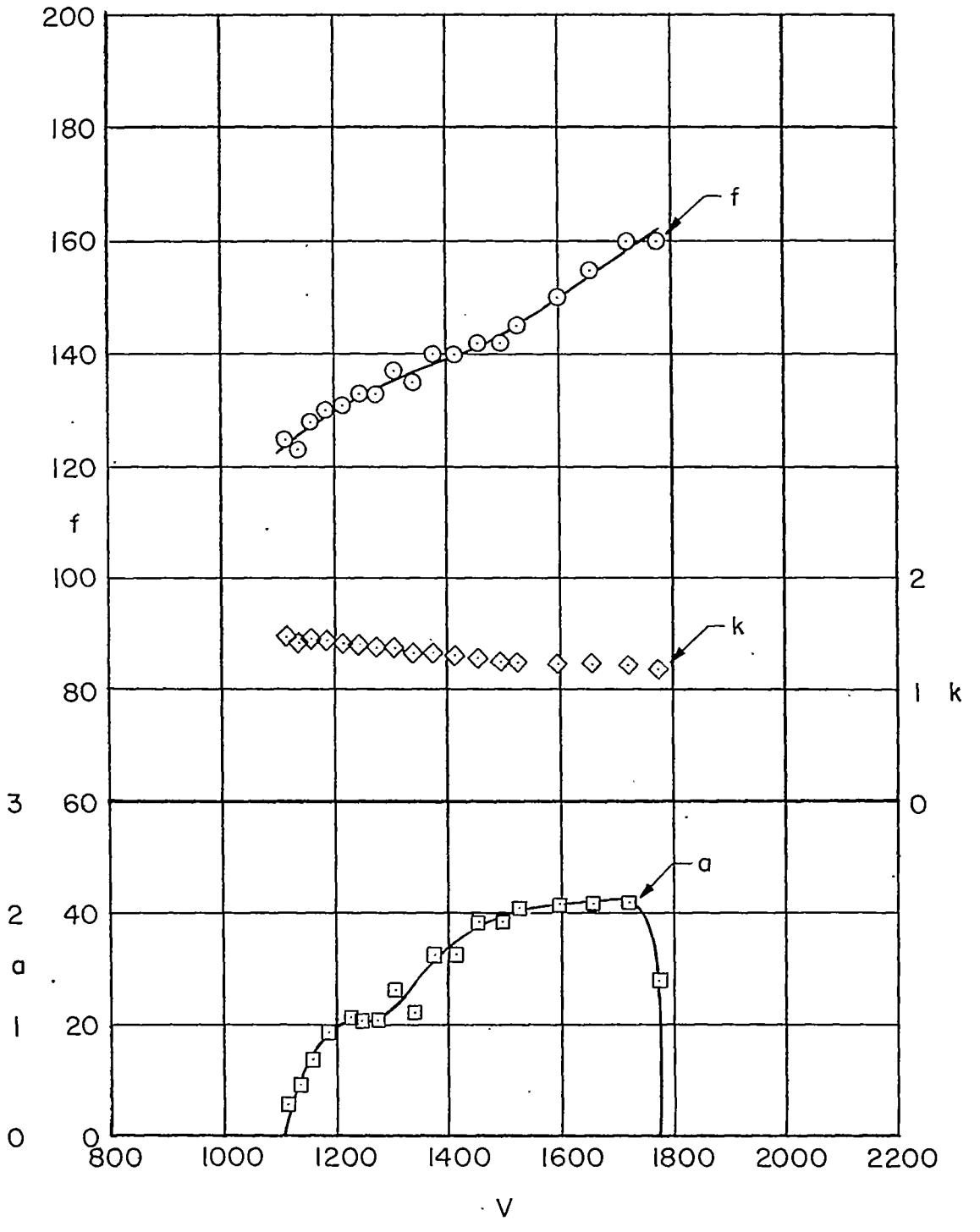

(a) Model 1 - delta wing (A = 3.07).

Figure 6.- Flutter frequency, amplitude, and reduced-frequency parameter plotted as functions of model speed. Flagged symbols indicate power-on flight.

[redacted]

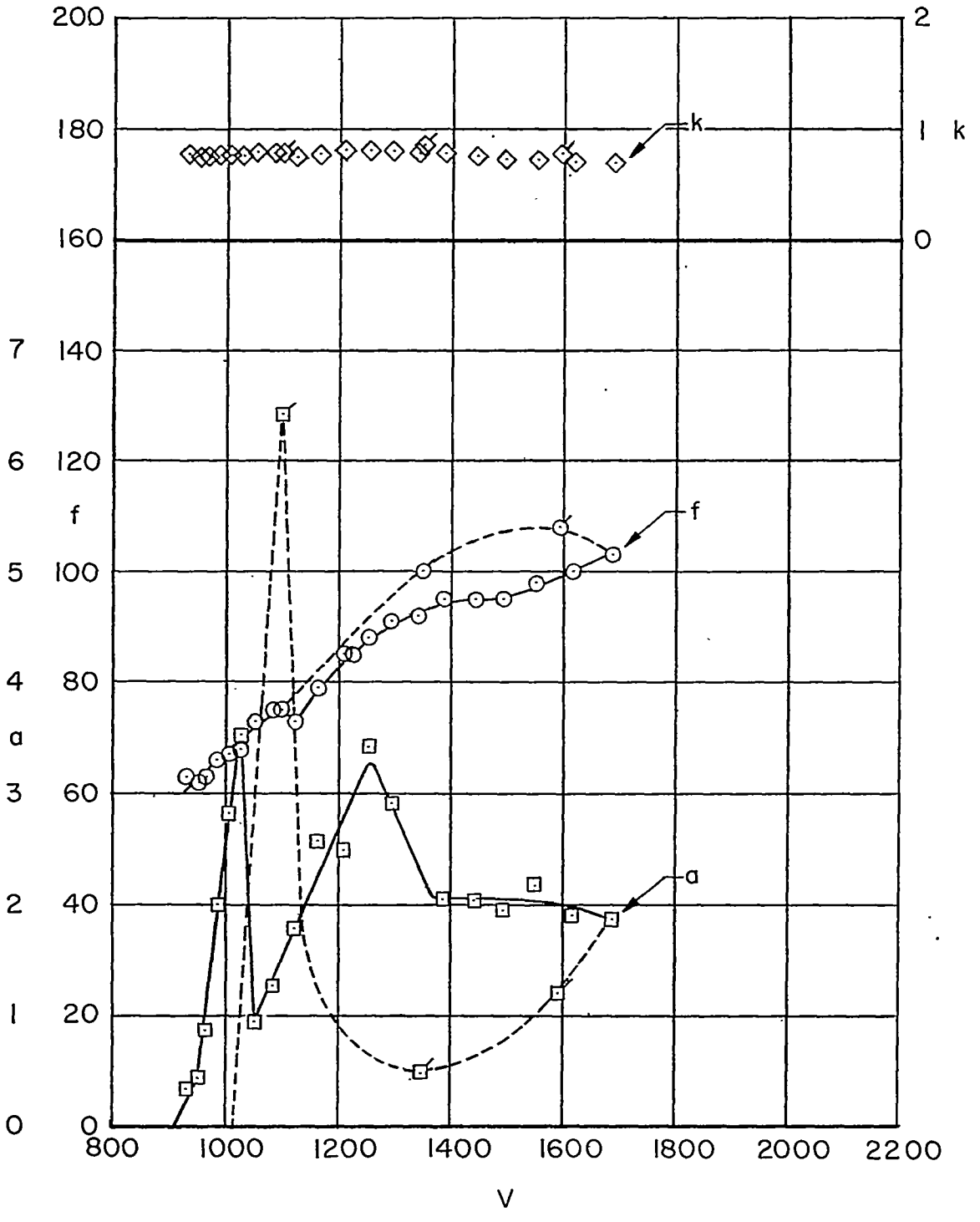

(b) Model 2 - delta wing (A = 4.0).

Figure 6.- Continued.

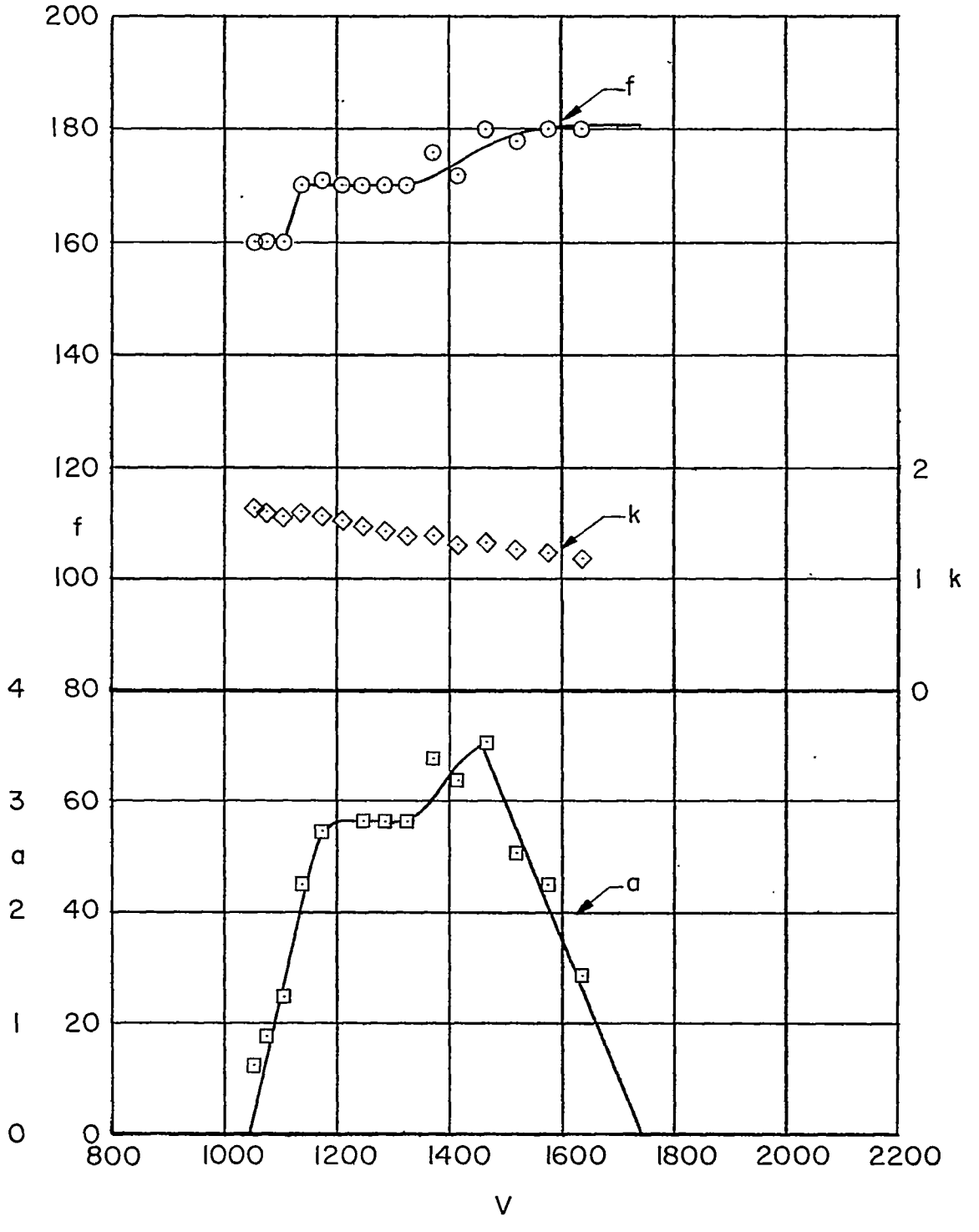

(c) Model 3 - diamond wing (A = 2.31).

Figure 6.- Continued.

[redacted]

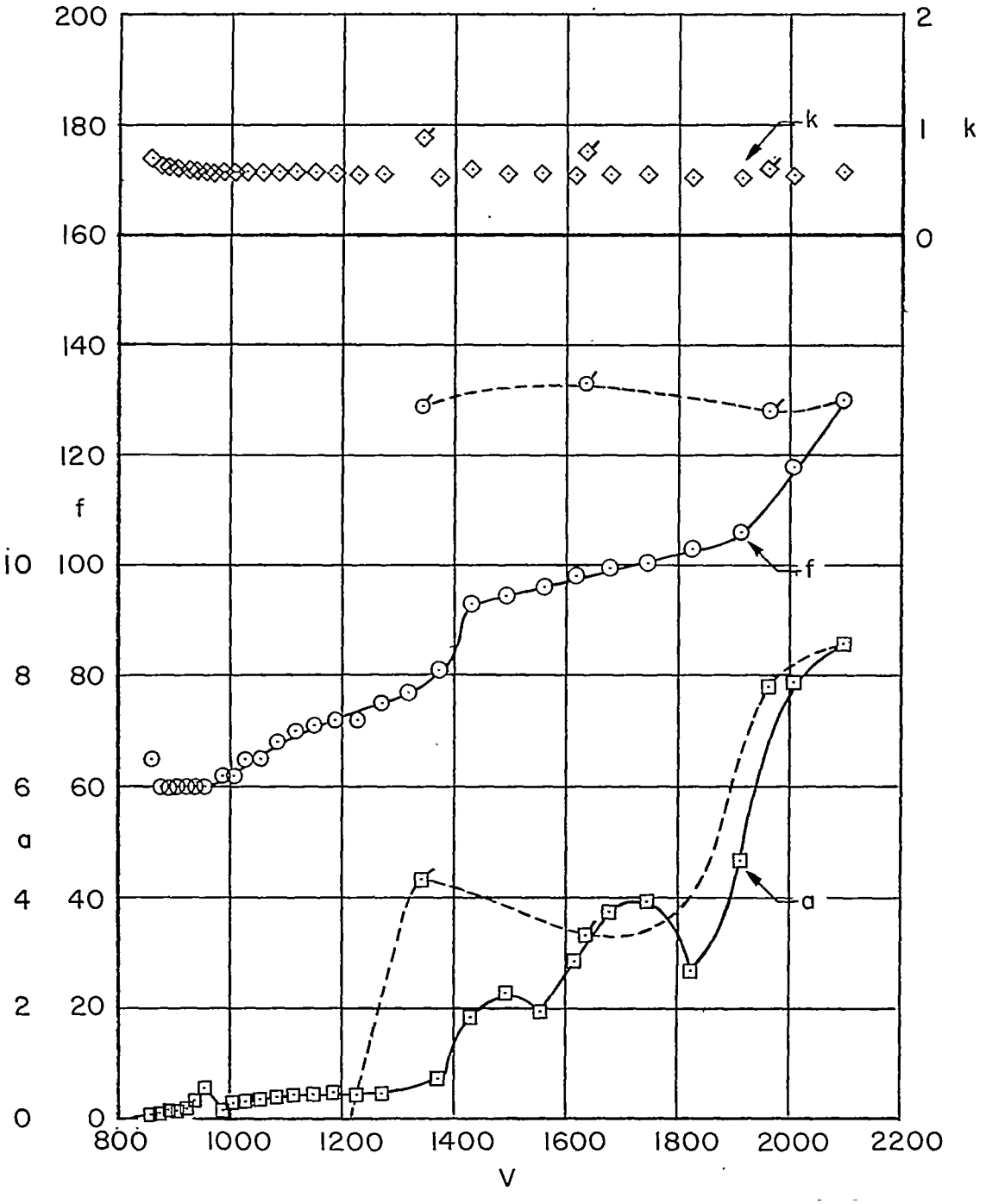

(d) Model 4 - diamond wing (A = 3.07).

Figure 6.- Continued.

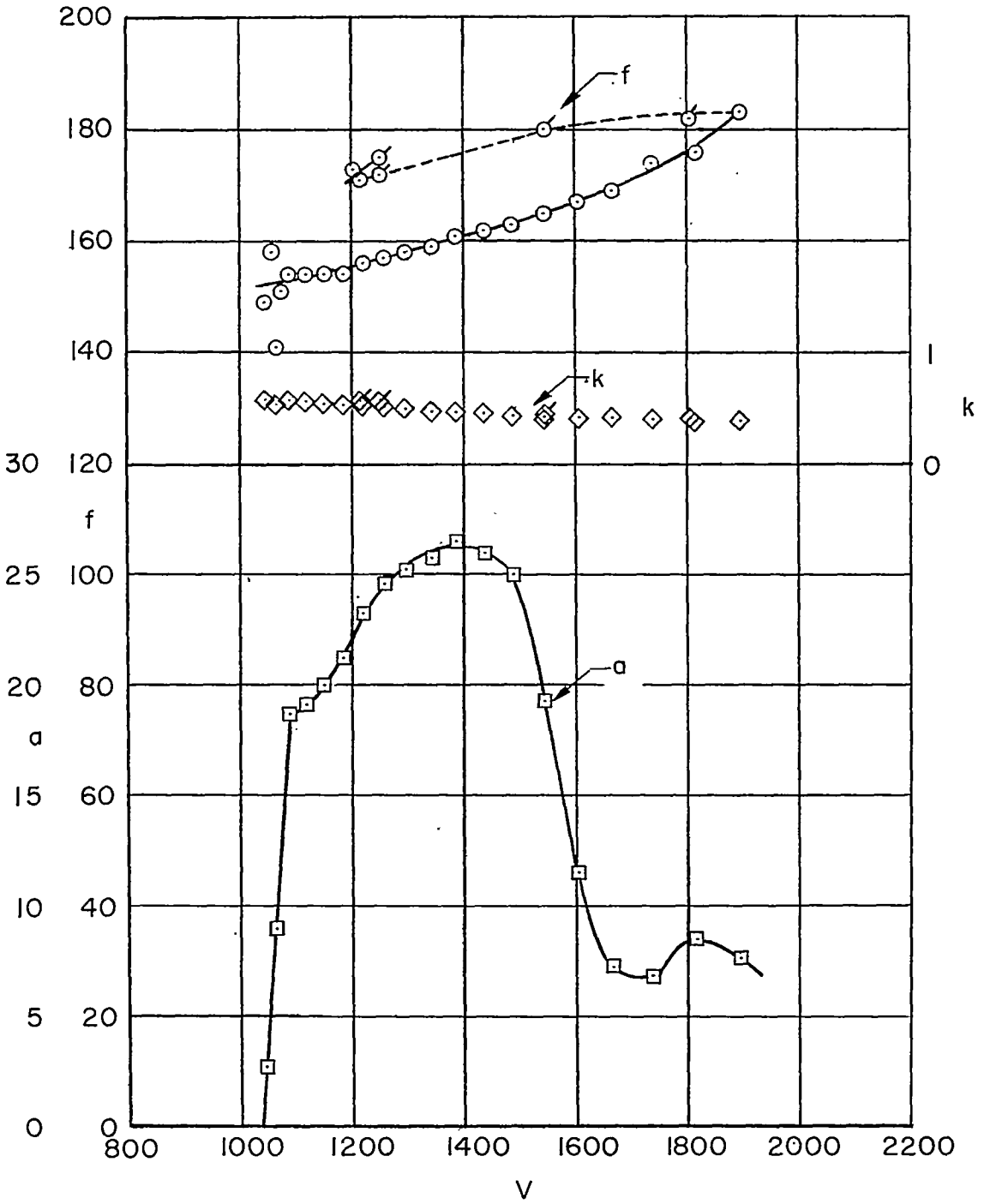

(e) Model 5 - arrow wing (A = 3.2).

Figure 6.- Concluded.

[redacted]

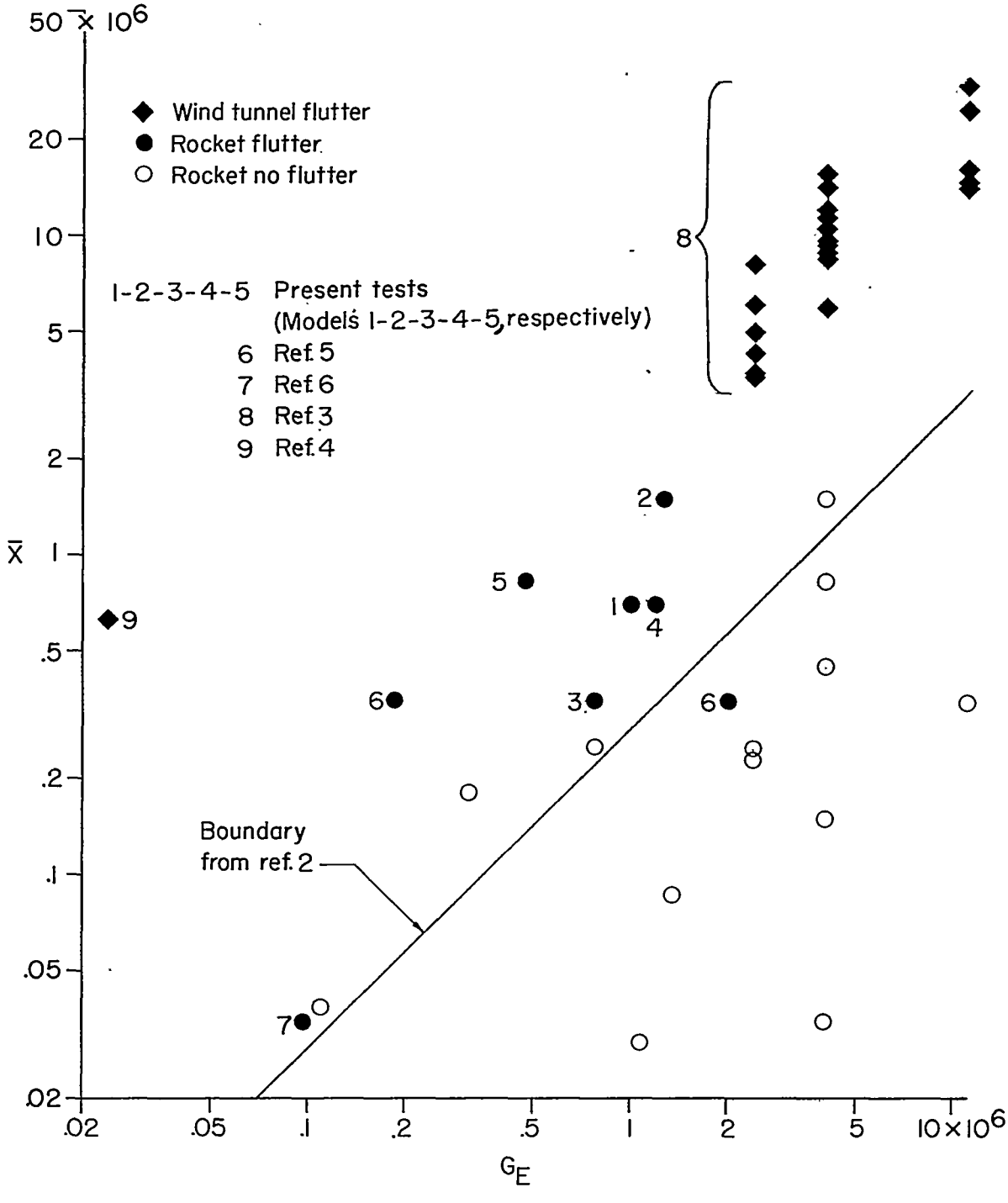

Figure 7.- Correlation of flutter data from rocket-propelled model and wind-tunnel tests of delta-, diamond-, and arrow-plan-form wings.

NACA-Langley - 4-4-55 - 325